Switching and Counting With Atomic Vapors in Photonic-Crystal Fibers

Thibault Peyronel, Michal Bajcsy, Sebastian Hofferberth, Vlatko Balic, Mohammad Hafezi, Qiyu Liang, Alexander Zibrov, Vladan Vuletic, and Mikhail D. Lukin

(Invited Paper)

***Abstract*—We review our recent experiments demonstrating a hollow-core photonic-crystal fiber loaded with laser-cooled atomic vapor as a system for all-optical switching with pulses containing few hundred photons. Additionally, we discuss the outlooks for improving the efficiency of this switching scheme and present preliminary results geared toward using the system as a photon-number resolving detector.**

***Index Terms*—All-optical switching, electromagnetically induced transparency, laser-cooled atoms in hollow-waveguides, photon number detection.**

I. Introduction

THE implementation of few-photon nonlinear optics has until now only been feasible in the context of cavity quantum electrodynamics (QED) when single-quantum emitters, such as neutral atoms or quantum dots, are placed inside narrow-band, high-finesse cavities. In these systems, the original nonlinearities of the optical medium created by the single emitter are amplified by the cavity finesse to the point where they can be controlled by the field of a single photon. Over the last decade, several experiments have demonstrated nonlinear optical phenomena with single intracavity photons [1]–[4]. However, the large nonlinearities achievable in these cavity-based systems come at the price of technological complexity, limitations imposed by cavity bandwidth, and often times substantial losses at the input and output of the cavity. The study presented here uses an alternative approach, which is based on coupling single emitters or ensembles of emitters to a propagating light field confined to an area comparable to the diffraction limit. This results in the electric field from a single photon being sufficiently large to cause nonlinear behavior on a single pass and without the environment of an optical cavity. Such tight confinement can be achieved either in free space by focusing the light beam with a large numerical aperture lens [5] or under conditions provided by a photonic waveguide. In particular, systems based on hollow core photonic crystal fibers [6], hollow antiresonant reflecting waveguides (ARROWs) [7], optical nanofibers [8], and nanostructure plasmonic waveguides allowing subdiffraction propagation [9] have all been actively explored in the last few years. Hollow core photonic crystal fibers (PCFs, also known as photonic bandgap fibers) that guide light through interference [10] instead of total internal reflection [11] are now available off the shelf and can be integrated with conventional optical fibers [12]. When filled with molecular gas, these fibers have shown significant enhancements in the efficiency of processes such as stimulated Raman scattering [13] and four-wave mixing [14]. Recently, both room-temperature and ultracold atoms have successfully been loaded into PCFs [15]–[17] and observations of electromagnetically induced transparency with less than a micro-Watt control field have been reported for the case of room temperature atoms [15].

Here, we review our experiments that demonstrate the strong coupling between light and laser-cooled atoms inside the hollow core PCF and allow us to implement all-optical switching controlled with light pulses containing as few as several hundred photons.

Manuscript received February 2, 2012; revised March 19, 2012; accepted April 12, 2012. This work was supported by MIT-Harvard Center for Ultracold Atoms, National Science Foundation, Defense Advanced Research Projects Agency, and Packard Foundation.

T. Peyronel, Q. Liang, and V. Vuletic are with the Physics Department, Massachusetts Institute of Technology, Cambridge, MA 02142 USA (e-mail: thibault.peyronel@gmail.com; Q_liang@mit.edu; vuletic@mit.edu).

M. Bajcsy was with School of Engineering and Applied Sciences, Harvard University, Cambridge, MA 02138 USA. He is currently with the Ginzton Laboratory, Stanford University, Stanford, CA 94305 USA (e-mail: bajcsy@stanford.edu).

S. Hofferberth was with the Physics Department, Harvard University, Cambridge, MA 02138 USA. He is now with Universität Stuttgart, Stuttgart 70569, Germany (e-mail: hofferberbe@physics.harvard.edu).

M. Hafezi was with the Physics Department, Harvard University, Cambridge, MA 02138 USA. He is now with the Joint Quantum Institute, University of Maryland, College Park, MD 20742 USA (e-mail: hafezi@umd.edu).

V. Balic was with the Physics Department, Harvard University, Cambridge, MA 02138 USA (e-mail: vlatko@balic.com).

A. Zibrov and M. D. Lukin are with the Physics Department, Harvard University, Cambridge, MA 02138 USA (e-mail: zibrov.alexander@gmail.com; lukin@physics.harvard.edu).

Color versions of one or more of the figures in this paper are available online at http://ieeexplore.ieee.org.

Digital Object Identifier 10.1109/JSTQE.2012.2196414

II. Atoms Inside the Fiber

The atoms are first laser-cooled and collected in a free-space magneto-optical trap and then transferred into a 30 mm long piece of hollow-core fiber (see Fig. 1) with a procedure described in detail in [18]. Once inside the fiber core, the cold atoms are confined in a red-detuned dipole trap [19]. The trap is created with an off-resonant beam guided by the fiber, and it prevents the atoms from colliding with the fiber wall. We probe the atoms, which form an approximately 1-cm long cloud inside the fiber core [18], by monitoring the transmission of very-low-power ($\sim$1 pW) probe beams that can be coupled into the fiber piece from either of its ends. After the probe beams emerge from the fiber, they are collimated by the coupling lenses and then

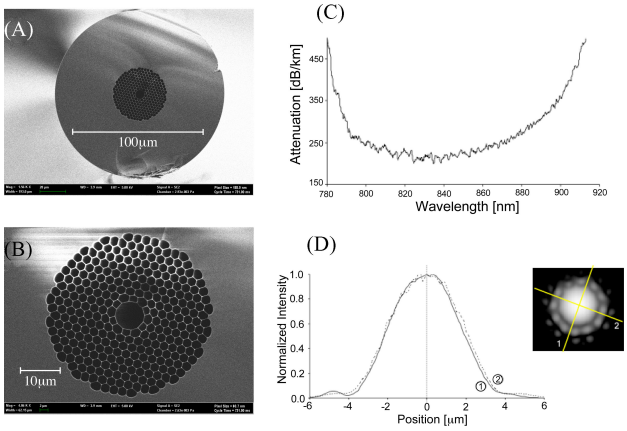

Fig. 1. (A) Scanning electron microscope (SEM) image of a cross section of the hollow-core photonic-crystal fiber from Blaze Photonics used in the experiment (model *HC-800-02*). (B) Detail of the photonic crystal region of the fiber with the hollow core in the center. Manufacturer's specifications of (C) losses of guided mode propagating in the fiber as a function of wavelength and (D) near field intensity distribution of the guided mode.

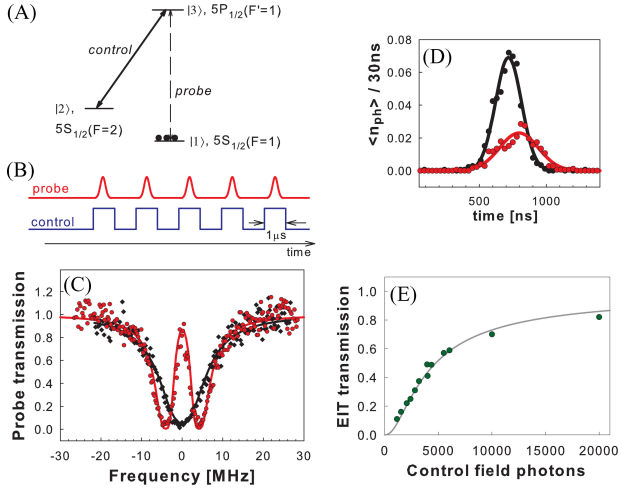

Fig. 2. (A) Atomic level scheme and the corresponding hyperfine states of rubidium^{87} used in the EIT demonstration. (B) Both probe and control field are broken into a set of ∼100 synchronized pulses sent through the fiber during the off-times of the dipole trap. (C) Transmission of the probe light through the fiber as a function of detuning from resonance in the presence of the control field (red data). The black data show probe transmission without the control field. (D) Individual probe pulse shape and delay. Here, $\langle n_{\rm ph}\rangle$ represents the average number of photons detected in a 30-ns time bin. The reference pulse (black) is obtained without the presence of atoms inside the fiber. The red pulse is delayed due to the group velocity reduction in the atomic medium under EIT conditions. (E) Observed transmission of the probe pulses on resonance as a function of average number of photons in the 1 μs control field pulse and the prediction (gray line) obtained by evaluating equation (2) in [24].

passed through a series of optical filters that separate the probe photons from other light beams coupled into the fiber during the experiments. Finally, the probes are coupled into single-mode fibers connected to single-photon counters. The use of single-mode fibers provides spatial filtering that ensures that only photons propagating in the guided mode of the PCF are detected. We calibrate the output signal of the single-photon counters by sending a beam with macroscopic power (∼1 mW) through the system in the absence of atoms and then reducing the power in this beam with a series of neutral density filters with precisely known attenuation factors.

When the frequency of the probe laser is scanned over an atomic resonance, we observe in the transmitted signal an approximately Lorentzian absorption line-shape from the atoms present inside the fiber:

$$T_{\rm nat} = \exp\left(-\frac{\rm OD}{1+4(\frac{\delta_p}{\Gamma_e})^2}\right) \tag{1}$$

where Γ_e is the linewidth of the excited atomic state and $\delta_p = \omega_p - \omega_0$ is the detuning of the probe laser from resonance. The optical depth OD is a figure of merit for the strength of the observed absorption. In general, OD depends on the atomic density integrated along the fiber, and the strength of the considered atomic transition. Since the atoms are confined within the optical trap created by the guided light inside the fiber, the radial extent of the atomic cloud is smaller than the beam area of the single-mode probe light beam propagating through the fiber. To get an accurate relation between optical depth and atomic density inside the fiber, we have to take into account the atoms' radial distribution in the probe beam. In particular, an atom at the edge of a beam experiences a smaller electric field and, therefore, absorbs less light than an atom on the beam's axis. Assuming a Gaussian beam with waist w_o and a radially symmetric atomic density $n(r,z)$, the expression for optical depth on resonance is

$$\mathrm{OD}_{\rm fiber} = \frac{2}{\pi w_o^2}\int_{L_{\rm cloud}} 2\pi \int_0^{r_{\rm core}} n(z,r) c_{\rm CG}^2 \sigma_o e^{-\frac{2r^2}{w_o^2}} r dr dz \tag{2}$$

where $\sigma_o = \frac{3\lambda^2}{2\pi}$ is the maximal atomic cross section, and $c_{\rm CG}$ is the Clebsch-Gordon coefficient for the specific atomic transition being used. In general, (2) reduces to a simple expression that shows that OD is proportional to the number of atoms $N_{\rm at}$ inside the fiber:

$$\mathrm{OD}_{\rm fiber} = \eta\, N_{\rm at}\, \frac{2c_{CG}^2\sigma_o}{\pi w_0^2}. \tag{3}$$

The prefactor η is given by the radial distribution of atoms in the fiber-confined cloud. The highest value of η corresponds to all atoms being localized on the axis of the fiber, in which case $\eta = 2$. In the case of a Gaussian radial density distribution with waist x_0, $n(r) = n_0 e^{-\frac{r^2}{2x_0^2}}$, $\eta = \frac{2(w_0/2)^2}{x_0^2+(w_0/2)^2}$. The optical depth of the atomic cloud inside the fiber is, thus, determined by the number and temperature of atoms inside the fiber. In particular, higher atomic temperatures lead to more axially delocalized cloud (increased x_0), which in turn results in decreased OD. Assuming an atomic temperature $T \sim 1$ mK and using the measured beam waist of guided light inside the fiber $w_0 = 1.9 \pm 0.2$ μm, ∼100 atoms inside the fiber create an optically dense medium (OD = 1) when probed at the transition with the highest Clebsch-Gordon coefficient.

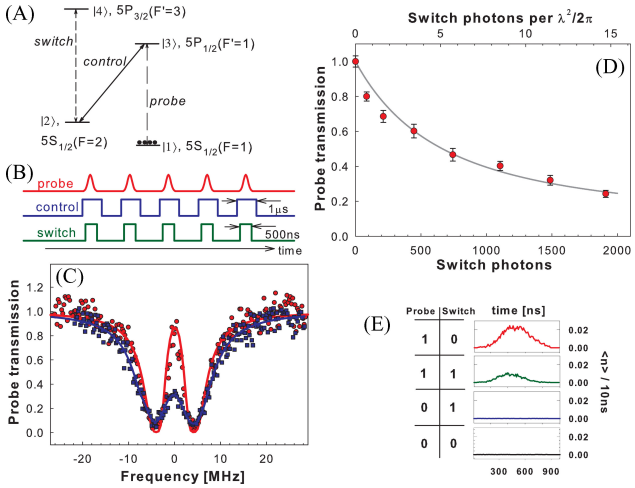

Fig. 3. (A) Atomic level scheme with corresponding hyperfine states of rubidium^{87} used in the experiment. (B) Probe, control and switch fields are broken into a set of $\sim$100 synchronized pulses sent through the fiber during the off times of the dipole trap. (C) Probe transmission through the fiber without (red) and with (blue) the switch field present. Solid lines are fits of (2) in [24]. (D) Observed transmission versus average number of switch photons per pulse. The solid gray line is the prediction based on (2) in [24]. The transmission is normalized to the EIT transmission in the absence of the switch photons. (E) Truth table of the switch, showing the detected photons in the output port of the switch system as a function of the presence of the probe and switch field pulses. Data are presented for probe pulses containing on average $\sim$2 photons and with $\sim 1/e$ attenuation of transmission in the presence of the switch photons.

III. All-Optical Switching

The mechanism used here for all-optical switching is based on electromagnetically induced transparency (EIT) [20], [21]. In this phenomenon, an atomic ensemble, which is originally opaque for a resonant probe beam, is changed to transparent with the help of a control beam. For this, we consider the 3-state Λ-configuration of atomic states shown in Fig. 2(A). In the presence of a strong control field, the weak probe field, resonant with the $|1\rangle \rightarrow |3\rangle$ transition, is transmitted without loss. The essence of EIT is the creation of a coupled excitation of probe photons and atomic spins ("dark-state polariton") [22] that propagates through the atomic medium with greatly reduced group velocity [23] and can be efficiently manipulated.

To demonstrate EIT, we first prepare the atoms in the $F = 1$ ground state, and then probe the medium with a linearly polarized probe tuned to the D1 $F = 1 \rightarrow F' = 1$ transition. In the absence of the control beam, the medium is completely opaque at resonance (Fig. 2(C), black data points). In contrast, when a copropagating control field resonant with the $F = 2 \rightarrow F' = 1$ transition is added, the atomic ensemble becomes transparent near the probe resonance (see Fig. 2(C), red data points). Fig. 2(D) shows the individual pulse shape and its transmission and delay due to reduced group velocity v_g inside the atomic medium. For a probe pulse of half-width t_p $\sim$150 ns, we observe a group delay t_d approaching 100 ns, corresponding to reduction of group velocity to $v_g \approx 3$ km/s. Finally, Fig. 2(E) shows the resonant probe transmission as a function of the average number of photons contained in each control field pulse. Due to the tight confinement of light provided by the PCF, control pulses containing $\sim 10^4$ photons are sufficient to achieve almost complete transparency of an otherwise opaque system.

An efficient nonlinear optical switch can be realized by adding to the EIT Λ-system a switch field coupling the state $|2\rangle$ to an excited state $|4\rangle$ [see Fig. 3(A)], as proposed by Harris and Yamamoto [25]. In this scheme, the switching photons interact with flipped atomic spins within the slow dark-state polariton, causing a simultaneous absorption of a probe and a switch photon [26]–[28].

In our experiment, an additional switching field resonant with the $F = 2 \rightarrow F' = 3$ transition of the D2 line of rubidium^{87} [see Fig. 3(A) and (B)] controls the transmission through the EIT medium. As shown in Fig. 3(C), in the absence of the switching field (red data), we observe high transmission of the probe beam on resonance due to EIT. When the switch field is turned ON, this transmission is reduced. The strength of the reduction depends on the switch field intensity, which, for a fixed switch pulse length, is determined by the number of photons contained in the switch pulse [see Fig. 3(D)]. Experimentally, we observe best switching results for switch pulses of length $t_s \approx t_p + t_d$. We find a 50% reduction of the initial transmission for a total number of $\sim$700 switch photons per pulse. Fig. 3(E) presents the truth table of our switch. In the case of no probe pulse (0/0 and 0/1 settings of the switch) only background noise from the control field is detected, which is orders of magnitude smaller than the single photon per probe pulse.

A detailed analysis of the behavior of our atomic medium can be found in [24]. However, for the relevant case of a resonant probe field, the transmission of the probe pulse can be approximated by

$$T = \frac{\exp\left(-N_s \left(\frac{\mu_s}{\mu_p}\right)^2 \frac{3}{\pi}\frac{\lambda^2}{A}\frac{t_d}{t_p+t_d}\right)}{\sqrt{1+\frac{16t_d^2}{\mathrm{OD}\,t_p^2}}}. \tag{4}$$

Here, N_s is the number of switch photons, we assumed that the Rabi frequency of the control field is much larger than that of the switching field, the decay rate of state $|3\rangle$ is approximately the same as of state $|4\rangle$, and we used $t_d = L/v_g \approx \frac{\mathrm{OD}\gamma_{13}}{|\Omega_c|^2}$, with L being the length of the medium.

For the investigated case of a relatively weak probe transition and resulting OD ≈ 3, the delay time is small (t_d–t_p) and the probe pulse is never fully stored inside the medium. If the OD is increased (either by improving the atom loading efficiency or using a stronger probe transition), $t_d \gg t_p$ and the whole probe pulse is contained inside the medium as a dark state polariton in a mostly atomic form. In this case, it follows from (4) that $N_s \sim \frac{A}{\lambda^2}$ switch photons attenuate the probe pulse by a factor of $1/e$.

IV. Outlooks for Switching Efficiency Improvements

Since the switching mechanism is based on a simultaneous absorption of a switch and a probe photon, the electric field envelopes of switch pulse and of the probe pulse have to overlap inside the atomic medium. To maintain this overlap despite the large mismatch between the propagation velocities of the two

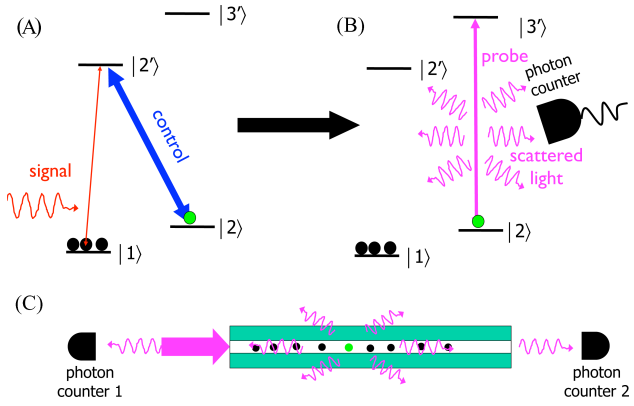

Fig. 4. *Photon counting*: (A) Photons are coherently stored in atomic ensemble as dark state polaritons and each photon results in a single collective excitation. (B) Ensemble is then probed with a detection laser on a cycling transition (i.e., from state $|3'\rangle$ the atom can spontaneously decay only into state $|2\rangle$), which allows scattering of multiple photons by a single excitation. (C) When the atomic ensemble is confined inside a hollow-core PCF, the scattered photons are collected and guided by the hollow fiber and detected with a photon counter. Alternatively, the presence of collective excitations can be detected by measuring the transmission of the fiber.

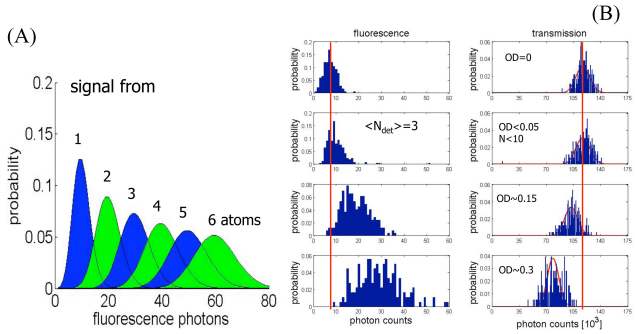

Fig. 5. (A) Effects of shot noise in detected photons on atom number resolution for $\alpha M_{\rm cycl} = 10$. (B) Collected fluorescence and measured transmission from fiber-confined atomic ensembles of various optical depths. For the probed transition, ~200 atoms result in OD ≈ 1 [18].

pulses, the switching pulse has to stay on during the whole time t_d the probe pulse is propagating in the medium. This in turn leads to an inefficient performance of the switch, as most of the area of the switching pulse will end up not overlapping with the probe pulse. Consequently, most of the switch photons needed to create a long switching pulse of required field intensity will go to waste. This inefficiency can be improved by matching the group velocities of the probe and switching pulses during their propagation through the atomic ensemble [29]. In this way, a full overlap between the two pulses can be maintained even when the switching pulse length is reduced to t_p, which in turn leads to a reduction of the number of switch photons needed. For t_p matched to the spectral width of the transparency window of the system, we then find that $N_s \sim \frac{A}{\lambda^2\sqrt{\rm OD}}$.

Alternatively, the efficiency of this switching scheme can potentially be further improved by using stationary-pulse techniques [30]. In this case, a standing wave control field from two counter-propagating beams forms an EIT Bragg grating in which the probe pulse can be completely stopped with nonvanishing photonic component. Application of this scheme inside the PCF has been proposed for single-photon-controlled switching through an interaction of single-photon stationary light pulses, with probability of interaction between two single photons scaling as $\sim {\rm OD}\frac{\lambda^2}{A}$ [31].

V. Atom and Photon Detection

In addition to all-optical switching, our system can be used to implement an efficient photon counting scheme proposed in [32] and [33]. This scheme combines photon storage [see Fig. 4(A)] [34], [35] with spin-flipped atom interrogation via a cycling transition as illustrated in Fig. 4(B). Practical limitations in realistic atomic systems arise from experimental imperfections that can transfer the atom into state $|1\rangle$ with nonzero probability during the interrogation stage. This restricts the number of photons that can be scattered from the stored excitation, which in turn requires the scattered light to be collected with certain minimum efficiency. Implementing the photon-counting scheme with an atomic ensemble confined inside a hollow-core fiber could potentially provide the necessary efficiency boost due to collection and guiding of the scattered photons by the fiber [see Fig. 4(C)]. A necessary step on such implementation is the detection of single atoms inside the hollow-core fiber as this would indicate the capability of the system to detect and resolve single photons stored in atomic ensembles. Here, we present initial experimental results of our study in this area.

When detecting small number of atoms inside the hollow fiber, the number of photons detected by the photon counter in Fig. 4 is given by

$$N_{\rm det} = N_{\rm sig} M_{\rm cycl} \alpha \tag{5}$$

where $N_{\rm sig}$ is the number of atoms inside fiber, $M_{\rm cycl}$ is the average number of photons that can be scattered by a single atom before the atom is lost by a transfer to state $|1\rangle$ or by being heated out of the trap, and α the overall detection efficiency of the scattered photons. This relation also works for the case of photon counting with $N_{\rm sig}$ being the number of photons stored in the atomic ensemble. α is the product of our atom-fiber cooperativity and of the detection efficiency for photons in the guided mode of the fiber. The atom-fiber cooperativity for an atom located at the center of the fiber (i.e., the probability for the atom to absorb a single photon in the mode of the fiber) is (3) 1.8% (we use linear-polarized light on the cycling $|5s_{1/2}, F = 2\rangle \rightarrow |5p_{3/2}, F = 3\rangle$ transition, because of the polarization properties of the PCF). From the optical theorem, it is equivalent to the probability for an atom inside the fiber to scatter a photon in one of the directions of the guided mode of the fiber [36]. We measure a cooperativity of 0.38% by comparing the transmission and back-scattering of resonant light out of the PCF for ensembles of ~100 atoms. This value is in excellent agreement with the one measured using incoherent population transfer in [18]. Although this number is compatible with a Gaussian distribution with temperature 1.6 mK, a more detailed probing of the resonant transitions inside the dipole trap point toward the fact that a significant fraction of the atoms seem to have a radially elliptical trajectory and do not contribute highly

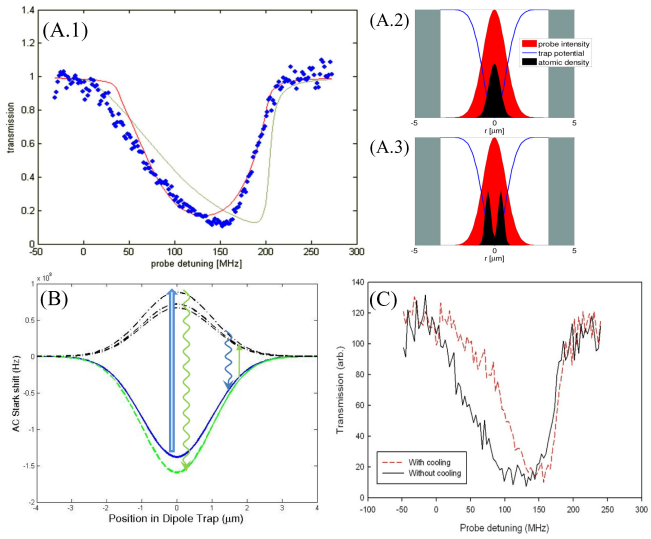

Fig. 6. (A.1) Probe absorption in the continuous dipole trap (blue dots). The data show a stronger ressemblance to the expected curves for a ring-like distribution (red, A.3) than for a thermalized cloud (green, A.2). (B) In-fiber cooling can be implemented by adding a blue detuned beam to our dipole trap. The ac-Stark shift as a function of the atom's radial position in the fiber-guided dipole trap plotted for the different Zeeman sublevels of the $|5s_{1/2}, F = 1\rangle$(continuous, blue), $|5s_{1/2}, F = 2\rangle$(dashed, green), and $|5p_{1/2}, F = 2\rangle$(dash-point, black) states in the presence of a 25 μW beam, blue-detuned by 8 GHz from the $|5s_{1/2}, F = 1\rangle \rightarrow |5p_{1/2}, F = 2\rangle$ transition. At the center of the trap, the blue-detuned light preferentially scatters the atoms out of $|F = 1\rangle$ (upward blue double arrow). When the atoms spontaneously decay back to $|F = 2\rangle$ (downward squiggly green arrow), their energy is reduced by the difference in Stark-shift between the two hyperfine ground states. A low-power repumper (upward green arrow) that works more efficiently at the edge of the trap than in the center because of the position-dependent ac-Stark shift, and spontaneous emission (downward blue squiggly arrow) recycle the atoms back into $|F = 1\rangle$ at a position away from the center of the trap, where the level-shift difference between the two ground states is smaller than it is on the axis of the fiber. (C) Probe absorption in the dipole trap with (black, continuous) and without (red, dashed) $\sim$1 ms of the cooling scheme described earlier. In the presence of cooling, the narrowed absorption profile results from the atoms being radially cooled to the bottom of the trap, although we also observe some loss of atoms out of the trap in the process.

to the atom-fiber cooperativity [see Fig. 6(A)]. Unlike the all-optical switch data obtained with modulated dipole trap [37], Fig. 6(A.1) plots the transmission of the atoms inside the fiber with the dipole trap turned ON continuously. The broadening and frequency shift of the atomic absorption originates from the ac-Stark shift [19] caused by the dipole trap. As the ac-Stark shift of each individual atom is determined by the intensity of the dipole trap at the atom's position, atoms located closest to the center of the fiber will experience the highest amount of ac-Stark shift. The frequency dependence of the absorption of the overall atomic ensemble then provides us with information about the radial distribution of the atoms inside the fiber. In particular, for atomic distribution from Fig. 6(A.2), we expect the absorption to follow the olive-green curve plotted in Fig. 6(A.1). However, the experimental data (blue circles) follows more closely the red curve in Fig. 6(A.1), which results from the radial distribution shown in Fig. 6(A.3). This agrees with classical single-particle trajectories for atoms rolling down a bottleneck-type potential created by the dipole trap at the entrance of the fiber and starting off-center with some initial azimuthal velocity, such as analyzed, for example, in [38]. Note that densities in the fiber are too low for the atomic ensemble to rethermalize. Combining the atom-fiber cooperativity with the quantum efficiency of our photon counters and coupling losses, our current setup is limited to $\alpha \sim 10^{-3}$.

The total number of photons $M_{\rm cycl}$ which an atom can scatter is limited by the off-resonant scattering to another state, especially inside the PCF where the clean circular polarization required for the $|5s_{1/2}, F = 2, mF = 2\rangle \rightarrow |5p_{3/2}, F = 3, mF = 3\rangle$ transition is not achievable because of birefringence and multimode effects. For the purpose of atom counting, the loss of atoms to the $|5s_{1/2}, F = 1\rangle$ state can be counteracted by periodic optical pumping. Another limiting factor to $M_{\rm cycl}$ is the lifetime of the atoms in the modulated dipole trap. The probing occurs during the off times of a modulated dipole trap as it is not possible to filter out dipole trap photons well enough to detect the low light level signal emanating from a few atoms. The lifetime in the modulated dipole trap is reduced to 4 ms at 1 MHz modulation rate due to parametric heating. Other heating mechanisms contribute to reducing the lifetime. If the atoms are probed unidirectionally in the fiber, the photon recoil accelerates the atoms, with two important consequences: the probe light is Doppler-shifted out of resonance, and the atoms rapidly escape the trap. We attribute the second effect to the mixing of the longitudinal and radial external degrees of freedom due to corrugations in the confining potential created by interference with the surface modes propagating at the core-cladding interface [39]. A clear signature of the longitudinal acceleration is the Doppler shift of the atoms and the effect can be counterbalanced by alternating probing phases with in-fiber longitudinal red-detuned molasses. Each scattering event also contributes one photon-recoil energy to the thermal energy of the atoms, due to the randomness of the emission process. The molasses can compensate the heating in the longitudinal direction. In the radial directions, the trap depth of $\sim$10 mK corresponds to $\sim 10^5$ times the thermal energy gained per scattering event. In the absence of any other heating mechanism and using a resonant probe at saturation intensity, $M_{\rm cycl}$ is restricted by the lifetime of the atoms in the modulated dipole trap to $\sim 10^4$.

The atom number (and eventually photon number) resolution in this system is limited by the shot noise of detected photons, and we get from (5) that the uncertainty in measured photon number would be

$$\Delta N_{\rm sig} = \frac{N_{\rm det}^{\frac{1}{2}}}{\alpha M_{\rm cycl}} = \left(\frac{N_{\rm sig}}{\alpha M_{\rm cycl}}\right)^{\frac{1}{2}}. \tag{6}$$

Fig. 5(A) plots the probabilities of detecting a particular number of photons for various number of atoms present in the fiber. For the parameters of our system, we see that the resolution of atom number becomes more difficult as the atom number increases over just a few.

Fig. 5(B) shows our initial experimental results. Here, we observed the fluorescence [photon counter 1 in Fig. 4(C)] and transmission [photon counter 2 in Fig. 4(C)] of atoms loaded into the fiber and probed on the cycling transition. The data are compared with the signal obtained from an empty fiber. We were able

to detect as few as ~ 10 atoms using the scattered light, when the atoms could not be observed in the transmission signal anymore. However, atoms disappear from the dipole trap after scattering only ~ 350 photons/atom. This value is independent of density, which excludes light assisted collisions as possible cause. It is also independent of trap depth, which excludes the simple heating mechanisms described earlier. We attribute this effect to the nonperfect linear polarization of the dipole trap, especially in the presence of surface modes. For a perfectly circular polarization, the dipole trap acts as a fictitious magnetic field and two successive Zeeman sublevels are shifted (for $|5s_{1/2}, F = 1\rangle$) by ~ 40 MHz for our parameters. At each turn-on of the dipole trap, the probe has reshuffled the population between the Zeeman sublevels. These energy fluctuations increase the thermal energy of the atoms by the Zeeman splitting at each cycle of the dipole trap. A few percent of circularly polarized light is enough to account for the atoms escaping the trap in the absence of radial cooling (the heating in the longitudinal direction is reduced by the optical molasses). Fig. 6(B) describes a way to cool the atoms without radial access by adding a weak blue-detuned (a few GHz to the $|5s_{1/2}, F = 2\rangle \rightarrow |5p_{1/2}, F = 1\rangle$ transition) and a weak repumper beam close to the free space resonance. As the radial position of an atom inside the fiber oscillates between the center and the edge of the dipole trap, the atom is transferred from $|F = 1\rangle$ ground state to $|F = 2\rangle$ ground state while passing through the center of the dipole trap, and repumped back into $|F = 1\rangle$ ground state when it reaches the edge of the dipole trap. For each depicted cycle, the atoms cool by an energy corresponding to the peak energy difference between the Stark-shifted hyperfine states. Fig. 6(C) displays preliminary results of this cooling method inside the PCF. After a few milliseconds of cooling, we observe a narrowing of the atomic absorption in the dipole trap (red dashed curve) compared to the original absorption profile (black solid curve), which indicates that the atoms have radially cooled to the bottom of the trap. Some losses occur during the process and we are currently working on improving this effect.

Successful realizations of photon number detection have been reported over the last decade with a variety platforms, and an excellent review of progress in this area can be found in [40]. However, because of challenges, such as low photon detection efficiencies, ability to resolve photon states with only a few photons, or the necessity to operate the detector at cryogenic temperatures, the implementation of a photon number resolving detector remains an open problem. This detection scheme, based on collecting the fluorescence from a cycling transition, has been theoretically predicted to achieve detection efficiency exceeding 99% and to distinguish states with ~ 50 photons [33]. While our system in its current form is not suitable for photon number detection, its weak spots can be fixed in the future. In particular, improvement of the atom-fiber cooperativity by an order of magnitude would allow robust photon number resolution. This could be achieved by in part by additional cooling and increased confinement of the atoms inside the fiber, but most directly by using a hollow waveguide with smaller diameter of the guided mode, such as the one demonstrated in [41].

VI. Conclusion

With the fiber acting as a guide for both photons and atoms, the photons can interact with an optically dense atomic ensemble without being limited by diffraction. This makes the system an excellent candidate for nonlinear optics at very low light levels [24], while the large optical depth achievable in this system [18] makes it ideally suited for the implementation of schemes for enhancing optical nonlinearities and creating effective photon–photon interactions [31], [42]–[46]. Finally, while the experiments discussed here were performed in a vacuum chamber containing a piece of hollow-core PCF, recent developments in the design and fabrication of integrated hollow optical waveguides [47], [48] open the possibilities for developing this system into a scalable on-chip architecture.

Acknowledgment

The authors would like to thank Y. Chu and D. Brown for their technical assistance during the early stages of the experiment. T. Peyronel, M. Bajcsy, S. Hofferberth contributed equally to this work.

References

[1] K. M. Birnbaum, A. Boca, R. Miller, A. D. Boozer, T. E. Northup, and H. J. Kimble, "Photon blockade in an optical cavity with one trapped atom," *Nature*, vol. 436, no. 7047, pp. 87–90, Jul. 2005.

[2] T. Wilk, S. C. Webster, A. Kuhn, and G. Rempe, "Single-atom single-photon quantum interface," *Science*, vol. 317, no. 5837, pp. 488–490, 2007.

[3] I. Fushman, D. Englund, A. Faraon, N. Stoltz, P. Petroff, and J. Vuckovic, "Controlled phase shifts with a single quantum dot," *Science*, vol. 320, no. 5877, pp. 769–772, 2008.

[4] B. Dayan, A. S. Parkins, T. Aok, E. Ostby, K. Vahala, and H. Kimble, "A photon turnstile dynamically regulated by one atom," *Science*, vol. 319, no. 5866, pp. 1062–1065, 2008.

[5] J. Beugnon, C. Tuchendler, H. Marion, A. Gaëtan, Y. Miroshnychenko, Y. R. P. Sortais, A. M. Lance, M. P. A. Jones, G. Messin, A. Browaeys, and P. Grangier, "Two-dimensional transport and transfer of a single atomic qubit in optical tweezers," *Nature Phys.*, vol. 3, no. 10, pp. 696–699, 2007.

[6] R. Cregan, B. Mangan, J. Knight, T. Birks, P. Russell, P. Roberts, and D. Allan, "Single-mode photonic band gap guidance of light in air," *Science*, vol. 285, no. 5433, pp. 1537–1539, 1999.

[7] D. Yin, H. Schmidt, J. P. Barber, and A. R. Hawkins, "Integrated arrow waveguides with hollow cores," *Opt. Express*, vol. 12, pp. 2710–2715, 2004.

[8] L. M. Tong, R. R. Gattass, J. B. Ashcom, S. L. He, J. Y. Lou, M. Y. Shen, I. Maxwell, and E. Mazur, "Subwavelength-diameter silica wires for low-loss optical wave guiding," *Nature*, vol. 426, pp. 816–819, 2003.

[9] R. M. Dickson and L. A. Lyon, "Unidirectional plasmon propagation in metallic nanowires," *J. Phys. Chem. B*, vol. 104, pp. 6095–6098, Jun. 2000.

[10] J. D. Joannopoulos, R. D. Meade, and J. N. Winn, *Photonic Crystals: Molding the Flow of Light*. Princeton, NJ: Princeton Univ. Press, 1995.

[11] B. E. A. Saleh and M. C. Teich, *Fundamentals of Photonics*, 2nd ed. New York: Wiley-Interscience, 1997.

[12] F. Benabid, F. Couny, J. C. Knight, T. A. Birks, and P. S. Russell, "Compact, stable and efficient all-fibre gas cells using hollow-core photonic crystal fibres," *Nature*, vol. 434, pp. 488–491, Jan. 2005.

[13] F. Benabid, J. Knight, G. Antonopoulos, and P. Russell, "Stimulated raman scattering in hydrogen-filled hollow-core photonic crystal fiber," *Science*, vol. 298, no. 5592, pp. 399–402, 2002.

[14] S. O. Konorov, A. B. Fedotov, and A. M. Zheltikov, "Enhanced four-wave mixing in a hollow-core photonic-crystal fiber," *Opt. Lett.*, vol. 28, pp. 1448–1450, 2003.

[15] S. Ghosh, A. R. Bhagwat, C. K. Renshaw, S. Goh, A. L. Gaeta, and B. J. Kirby, "Low-light-level optical interactions with rubidium vapor in a photonic band-gap fiber," *Phys. Rev. Lett.*, vol. 97, no. 2, 2006.

[16] T. Takekoshi and R. J. Knize, "Optical guiding of atoms through a hollow-core photonic band-gap fiber," *Phys. Rev. Lett*., vol. 98, no. 21, p. 210404, 2007.
[17] C. A. Christensen, S. Will, M. Saba, G.-B. Jo, Y.-I. Shin, W. Ketterle, and D. Pritchard, "Trapping of ultracold atoms in a hollow-core photonic crystal fiber," *Phys. Rev. A*, vol. 78, no. 3, p. 033429, 2008.
[18] M. Bajcsy, S. Hofferberth, T. Peyronel, V. Balic, Q. Liang, A. S. Zibrov, V. Vuletic, and M. D. Lukin, "Laser-cooled atoms inside a hollow-core photonic-crystal fiber," *Phys. Rev. A*, vol. 83, p. 063830, 2011.
[19] R. Grimm, M. Weidemuller, and Y. Ovchinnikov, "Optical dipole traps for neutral atoms," *Adv. Atom., Molec., Opt. Phys*., vol. 42, pp. 95–170, 2000.
[20] S. Harris, "Electromagnetically induced transparency," *Phys. Today*, vol. 50, pp. 36–42, 1997.
[21] M. Fleischhauer, A. Imamoğlu, and J. Marangos, "Electromagnetically induced transparency: Optics in coherent media," *Rev. Mod. Phys*., vol. 77, p. 633, 2005.
[22] M. Fleischhauer and M. D. Lukin, "Dark-state polaritons in electromagnetically induced transparency," *Phys. Rev. Lett*., vol. 84, pp. 5094–5097, 2000.
[23] L. Hau, S. Harris, Z. Dutton, and C. Behroozi, "Light speed reduction to 17 metres per second in an ultracold atomic gas," *Nature*, vol. 397, no. 6720, pp. 594–598, 1999.
[24] M. Bajcsy, S. Hofferberth, V. Balic, T. Peyronel, M. Hafezi, A. S. Zibrov, V. Vuletic, and M. D. Lukin, "Efficient all-optical switching using slow light within a hollow fiber," *Phys. Rev. Lett*., vol. 102, p. 203902, 2009.
[25] S. Harris and Y. Yamamoto, "Photon switching by quantum interference," *Phys. Rev. Lett*., vol. 81, p. 3611, 1998.
[26] M. Yan, E. Rickey, and Y. Zhu, "Observation of absorptive photon switching by quantum interference," *Phys. Rev. A*, vol. 64, p. 041801(R), 2001.
[27] D. Braje, V. Balic, G. Yin, and S. Harris, "Low-light-level nonlinear optics with slow light," *Phys. Rev. A*, vol. 68, p. 041801(R), 2003.
[28] Y. Chen, Z. Tsai, Y. Liu, and I. Yu, "Low-light-level photon switching by quantum interference," *Opt. Lett*., vol. 30, p. 3207, 2005.
[29] M. Lukin and A. Imamoğlu, "Nonlinear optics and quantum entanglement of ultraslow single photons," *Phys. Rev. Lett*., vol. 84, p. 1419, 2000.
[30] M. Bajcsy, A. S. Zibrov, and M. D. Lukin, "Stationary pulses of light in an atomic medium," *Nature*, vol. 426, pp. 638–641, 2003.
[31] A. André, M. Bajcsy, A. S. Zibrov, and M. D. Lukin, "Nonlinear optics with stationary pulses of light," *Phys. Rev. Lett*., vol. 94, no. 6, p. 063902, 2005.
[32] A. Imamoğlu, "High efficiency photon counting using stored light," *Phys. Rev. Lett*., vol. 89, no. 16, p. 163602, 2002.
[33] D. James and P. Kwiat, "Atomic-vapor-based high efficiency optical detectors with photon number resolution," *Phys. Rev. Lett*., vol. 89, p. 183601, 2002.
[34] D. F. Phillips, A. Fleischhauer, A. Mair, R. L. Walsworth, and M. D. Lukin, "Storage of light in atomic vapor," *Phys. Rev. Lett*., vol. 86, pp. 783–786, 2001.
[35] C. Liu, Z. Dutton, C. H. Behroozi, and L. Hau, "Observation of coherent optical information storage in an atomic medium using halted light pulses," *Nature*, vol. 409, pp. 490–493, 2001.
[36] H. Tanji-Suzuki, I. Leroux, M. Schleier-Smith, M. Cetina, A. Grier, J. Simon, and V. Vuletic, "Interaction between atomic ensembles and optical resonators: Classical description," *Adv. At. Mol. Opt. Phys*., vol. 60, pp. 201–237, 2011.
[37] M. Bajcsy, "Novel systems and techniques for nonlinear optics at low light levels," Ph.D. dissertation, School of Engineering and Applied Sciences, Harvard Univ., Cambridge, MA, Dec. 2009.
[38] J. Poulin, P. S. Light, R. Kashyap, and A. N. Luiten, "Optimized coupling of cold atoms into a fiber using a blue-detuned hollow-beam funnel," *Phys. Rev. A*, vol. 84, p. 053812, 2011.
[39] J. West, C. Smith, N. Borrelli, D. Allan, and K. Koch, "Surface modes in air-core photonic band-gap fibers," *Opt. Express*, vol. 12, pp. 1485–1496, 2012.
[40] M. D. Eisaman, J. Fan, A. Migdal, and S. V. Polyakov, "Invited review article: Single-photon sources and detectors," *Rev. Sci. Instrum*., vol. 82, pp. 071101-1–071101-25, 2011.
[41] G. S. Wiederhecker, C. M. B. Cordeiro, F. Couny, F. Benabid, S. A. Maier, J. C. Knight, C. H. B. Cruz, and H. L. Fragnito, "Field enhancement within an optical fibre with a subwavelength air core," *Nature Photon*., vol. 1, p. 115, 2007.
[42] M. Fleischhauer, J. Otterbach, and R. G. Unanyan, "Bose-einstein condensation of stationary-light polaritons," *Phys. Rev. Lett*., vol. 101, p. 163601, 2008.
[43] D. Chang, V. Gritsev, G. Morigi, V. Vuletic, M. Lukin, and E. Demler, "Crystallization of strongly interacting photons in a nonlinear optical fiber," *Nature Phys*., vol. 4, pp. 884–889, 2008.
[44] J. Otterbach, R. G. Unanyan, and M. Fleischhauer, "Confining stationary light: Dirac dynamics and klein tunneling," *Phys. Rev. Lett*., vol. 102, p. 063602, 2009.
[45] J. Otterbach, J. Ruseckas, R. G. Unanyan, and G. Juzeliūnas, M. Fleischhauer, "Effective magnetic fields for stationary light," *Phys. Rev. Lett*., vol. 104, p. 033903, 2010.
[46] A. V. Gorshkov, J. Otterbach, E. Demler, M. Fleischhauer, and M. D. Lukin, "Photonic phase gate via an exchange of fermionic spin waves in a spin chain," *Phys. Rev. Lett*., vol. 105, p. 060502, 2010.
[47] W. Yang, D. B. Conkey, B. Wu, D. Yin, A. R. Hawkins, and H. Schmidt, "Atomic spectroscopy on a chip," *Nature Photon*., vol. 1, p. 331, 2007.
[48] Q. M. Quan, I. Bulu, and M. Loncar, "Broadband waveguide QED system on a chip," *Phys. Rev. A*, vol. 80, p. 011810, 2009.

Thibault Peyronel is currently working toward the Ph.D. degree in the Physics Department, Massachusetts Institute of Technology, Cambridge, MA.

Michal Bajcsy received the Ph.D. degree in applied physics from Harvard University, Cambridge, MA, in 2010.

He is currently a Postdoctoral Scholar in the Ginzton Laboratory at Stanford University, Stanford, CA.

Sebastian Hofferberth received the Ph.D. degree in physics from the Universität Heidelberg, Heidelberg, Germany, in 2007.

He spent his Postdoctoral years at Harvard and MIT at the Center for Ultracold Atoms and is now at Universität Stuttgart, Stuttgart, Germany.

Vlatko Balic received the Ph.D. degree in physics from Stanford University, Stanford, CA. He spent two years as a Postdoctoral Researcher at Harvard and MIT at the Center for Ultracold Atoms and currently works for a start-up in New York, NY.

Mohammad Hafezi received the Ph.D. degree in physics from Harvard University, Cambridge, MA, in 2010.

He is currently a Research Associate at Joint Quantum Institute, University of Maryland, College Park.

Qiyu Liang is currently working toward the Ph.D. degree in the Physics Department, Massachusetts Institute of Technology, Cambridge, MA.

Alexander Zibrov is currently a Researcher at the MIT-Harvard Center for Ultracold Atoms, Harvard University, Cambridge, MA. He previously worked at the Harvard-Smithsonian Center for Astrophysics in Cambridge, MA, Department of Physics and Institute for Quantum Studies at the Texas A&M University, College Station, TX, and at the National Institute of Standards and Technology in Boulder, CO. He received the Ph.D. degree from the Lebedev Institute of Physics in Moscow, Russia.

Vladan Vuletic received the Ph.D. degree from Ludwig-Maximilians-Universität München, Munich, Germany.

He is a Professor of physics at the Massachusetts Institute of Technology, Cambridge, MA.

Mikhail D. Lukin received the Ph.D. degree from the Texas A&M University, College Station.

He is a Professor of physics at Harvard University, Cambridge, MA.